Correia, L.; Sena-Cruz, J.; Michels, J.; França, P.; Pereira, E.; Escusa, G. (2017) "Durability of RC slabs strengthened with prestressed CFRP laminate strips under different environmental and loading conditions." Composites Part B, 125: 71–88. DOI: 10.1016/j.compositesb.2017.05.047

Durability of RC slabs strengthened with prestressed CFRP laminate strips under different environmental and loading conditions

Luís Correia [a], José Sena-Cruz [a*], Julien Michels [b,c], Paulo França [d], Eduardo Pereira [a], Gonçalo Escusa [a]

[a] ISISE, Dept. of Civil Engineering, Univ. of Minho, Azurém, 4800-058 Guimarães, Portugal

[b] Structural Engineering Research Laboratory, Swiss Federal Laboratories for Materials Science and Technology (Empa), Überlandstrasse 129, 8600 Dübendorf, Switzerland

[c] re-fer AG, Oelistrase 6, 6440 Brunnen, Switzerland[d] CEris, ICIST and CCCEE, University of Madeira, Colégio dos Jesuítas, Portugal

* corresponding author: e-mail: jsena@civil.uminho.pt; tel.: (+351) 253 510 200; fax.: (+351) 253 510 217

Abstract:

Over the last decades, researchers have been studying fibre reinforced polymer (FRP) materials and their advantages in retrofitting of existing structures. The externally bonded reinforcement (EBR) technique is the most common practice in improving existing reinforced concrete (RC) structures with carbon FRP (CFRP) materials. In this regard, several additional advantages have been reported to the use of prestressed CFRP materials, mainly strips. However, the experience with RC strengthening using prestressed EBR-CFRP materials is still limited. Some concerns regarding the efficiency of the technique still exist, especially the durability and the long-term behaviour.

This work aims at contributing to the knowledge on durability of RC slabs strengthened with prestressed CFRP laminate strips according the EBR technique. The durability was studied by exposing strengthened RC specimens to the following environments for approximately 8 months: (i) reference environment – specimens kept in a climatic chamber at 20 ºC; (ii) water immersion in tank at 20 ºC of temperature; (iii) water immersion in tank with 3.5% of dissolved chlorides at 20 ºC of temperature; and (iv) wet/dry cycles in a tank with a water temperature of 20 ºC. Additionally, half of the specimens were subjected to sustained loading at a load level of 1/3 of the ultimate load, with the occurrence of cracking. After the exposure period the slabs were monotonically tested up to failure by using a four-point bending test configuration.

The results showed that the environmental conditions and the sustained loading, separately or combined, led in general to slight losses of performance and ductility. Although these losses were subtle, considering that the tests were carried out for 8 months, clear indications are given towards the importance of conducting similar tests

for longer periods. The results obtained showed that the procedures implemented to assess the durability of the strengthening systems were sensitive to the most relevant deterioration mechanisms and their impact on the mechanical properties of the specimens. Therefore, these procedures may well contribute for the future establishment of standardized test programmes for the assessment of the durability of prestressed CFRP strengthening systems.

Keywords:

EBR; durability; long-term behaviour; RC structures.

1. Introduction

Fibre-reinforced polymers (FRP) have been used to strengthen reinforced concrete (RC) structures because of their numerous advantages over conventional materials, such as higher strength and fatigue life, less susceptibility to corrosion and greater resistance against aggressive environments, as reported in the literature [1-7]. Generally, the Carbon FRP (CFRP) reinforcement materials are applied according to the externally bonded reinforcement (EBR) technique. If the FRP material is prestressed, a greater portion of its tensile capacity is utilized, consequently the use of its properties is more effective. Several advantages of using prestressed FRPs for RC structural strengthening have been reported in the literature over the last decades, such as the reduction of crack width and deflection, as well as the increase of the ultimate capacity and of the resistance to shear/fatigue brittle failure [3, 6-9]. The FRP strip can be directly prestressed (i) against the structure itself, (ii) against an independent system or it can be (iii) indirectly prestressed by cambering the structure upward. Prestressing against the structure itself does not require the use of heavy equipment, which makes this method more versatile and viable for *in situ* applications. For the case of (i) and (ii) special anchorage systems for fixing the ends of the prestressed FRP reinforcement are required. These end-anchorages are responsible for transferring the shear stresses from the reinforcement into the concrete substrate, allowing greater levels of prestressing, increasing the element's ductility and avoiding the premature failure by FRP pealing-off [3, 7, 10]. Literature already covers several studies on the short-term behaviour of RC elements strengthened with prestressed FRP where the focus was on (i) the development of the anchorage systems [1, 7, 11, 12] and on (ii) the service and ultimate behaviour [7, 11, 13, 14]. However, the technology is still regarded as novel and some topics still deserve attention, such as the durability and long-term behaviour.

The understanding of the long-term performance and durability of retrofitted structures is essential for structural safety. Other industry sectors (e.g. automotive, marine, industrial and aerospace) have been showing successful use of FRPs and epoxy adhesives for mass production of mechanical and structural components. However these results do not find direct translation into civil infrastructures applications, mainly because there are critical differences in loading, environmental exposures and the specific types of material/processes used in these applications [6]. External reinforcement may be subjected to a wide variety of environmental conditions such as for instance moisture cycling. The presence of water in materials like steel, concrete, epoxy resins and FRP materials can cause their degradation. In general, within a CFRP/epoxy/concrete system, concrete is the weakest link. Usually its tensile strength governs the structural failure by strip debonding. However, with the penetration of various environmental agents (e.g. water), failure mechanisms may change. Especially the behaviour of the epoxy resin, which can considerably influence the overall performance of the strengthening system. The absorption of water by the epoxy resin may vary depending on its degree of curing, structure and temperature. The moisture uptake by the epoxy adhesives can lead to physical and chemical alterations, leading to the reduction of their glass transition temperature and to their plasticization through hydrolysis (and consequently, to a reduction of their stiffness and of their ultimate strength) [15]. Also the absorption of water by FRPs at the fibre-matrix interface leads to the degradation of strength and consequently to the potential loss of structural integrity. Furthermore, the presence of salt water can accelerate the deterioration process due to the osmotic pressure effect [6] .

An experimental study [16] on the effect of moisture and salt water (NaCl) on the durability of FRP-based strengthening systems has shown that the maximum moisture uptake by carbon pultruded strips is significantly lower than in the wet layup systems. The authors also studied the bond performance of FRP systems after 2 years of exposure to five environments including the immersion in salt water and the immersion in deionized water. Results showed that the immersion in salt-water can produce higher reduction on bond strength (65% for carbon pultruded strips) than other environmental conditions like immersion in deionized water (38% for carbon pultrude strips).

Omran and El-Hacha [17] conducted an investigation on the assessment of the effects of sustained load and freeze-thaw cyclic exposure (500 cycles) on the flexural behaviour of eight RC beams strengthened with prestressed CFRP strips according to the NSM technique. The results showed that the specimens exposed to the combined effect of freeze-thaw cycles and sustained loading (47% of the theoretical ultimate capacity of a non-prestressed NSM beam) had an average decrease in the yielding load, ultimate load and ductility of 18%, 24% and 19%, respectively. The authors also observed that, after being subjected to the combined effect of freeze-thaw

cycling and sustained loading, prestressed specimens failed by strip end debonding at the concrete-epoxy interface. Strip end debonding did not occur on non-prestressed beams.

The effect of room (22 °C) and low temperatures (-28 °C) combined with sustained load (50% of the strengthened beam capacity) on prestressed EBR-CFRP RC beams was also studied by El-Hacha *et al.* [18]. A total of eight beams were used in this experimental program (four per studied temperature: (i) one unstrengthened control beam, (ii) one strengthened beam, (iii) one strengthened beam subjected to its own weight for one year and (iv) one strengthened beam subjected to sustained load for one year). The following main conclusions were obtained: (i) the strengthening produced a considerable enhancement in stiffness and strength; (ii) the isolated effect of sustained load had no impact on the beams ultimate strength; (iii) the combined effect of sustained load and low temperatures reduced the ultimate strength of the beams by 8%.

Despite the recent research developments on the durability and long-term behaviour of prestressed RC elements with FRPs, the effects of environmental exposure (immersion in water, immersion in water with chlorides or wet/dry cycles with water) on RC elements strengthened with prestressed EBR CFRP laminates was not yet addressed by the scientific community.

The main objective of this research is to study the effect of different environmental conditions on the durability of RC slabs strengthened with prestressed CFRP laminates according to EBR technique. Two different types of anchorage systems were studied: (i) mechanical anchorage (MA), a system that fixes the laminate ends with metallic plates; and, (ii) gradient anchorage (GA), which uses the ability of the epoxy to cure faster at higher temperatures, allowing to gradually reduce the prestressing force over several consecutive sectors at the strip end. The experimental program is composed of twenty slabs, sixteen of which were exposed to four different environmental conditions, along with gravity loading for a period of eight months. Then, specimens were monotonically tested under displacement control up to failure by using a four-point bending test configuration. The observed performance of the tested RC slabs allowed several conclusions regarding the durability and overall performance of both anchorage systems.

2. Experimental Investigation

2.1. Experimental program, specimens and test configuration

The experimental program included twenty reinforced concrete (RC) slabs as presented in Table 1: (i) four control specimens (series T0); (ii) eight slabs subjected to distinct environmental conditions (labelled with the suffix _U); and, (iii) eight slabs subjected to the combined effect of environmental and loading conditions (labelled with the

suffix _C). Loading and the exposure to different environmental conditions lasted for approximately eight months. Four distinct environmental conditions were considered: (i) specimens subjected to laboratory premises with a controlled temperature of 20°C and relative humidity of 55% (series REF and T0); (ii) specimens immersed in tap water at 20ºC (series TW); (iii) specimens immersed in water at 20ºC with 3.5%[i] of chlorides (series CW); and, (iv) specimens subjected to wet/dry cycles in tap water at 20ºC and without chlorides (series WD). As it is shown in Table 1, all specimens are labelled with a generic denomination: X_Y_Z, where X indicates the type of anchorage (MA or GA), Y stands for the environmental action (REF, TW, CW and WD) and Z indicates the cracking state when the specimen is first exposed to the environmental condition (U for uncracked and C for cracked) or T0.

The geometry of the specimens and test configuration are presented in Fig. 1. The RC slabs were 2600 mm long, with a cross-section of 600 mm (width) by 120 mm (height). All slabs were reinforced with 5 steel bars of 8 mm of diameter (5Ø8) in the tension zone and 3Ø6 in the compression zone. The transverse reinforcement was composed of closed steel stirrups of Ø6 with 300 mm of longitudinal spacing. Strengthening was performed by using 2200 mm long CFRP laminate strips with a rectangular cross-section of 1.2 mm by 50 mm.

In order to assess the behaviour of all specimens in service and ultimate design conditions, monotonic tests up to failure were performed using a four-point bending scheme with the two forces imposed centrally at a distance of 300 mm from the mid-span section (see Fig. 1). This configuration resulted in a shear span of 900 mm, since the total span is equal to 2400 mm. All tests were carried out with a servo-controlled equipment under displacement control at the rate of 1.2 mm/min of the actuator cross-head displacement. The instrumentation included: (i) 5 linear variable differential transducers (LVDTs) to record the deflection along the longitudinal axis of the slab; (ii) a minimum of 6 strain gauges per slab to measure the strain variation in the CFRP laminate, concrete and steel reinforcement; (iii) one load cell to measure the applied load (F). As shown in Fig. 1, LVDT2, LVDT3 and LVDT4 (range of ±75 mm and a linearity error of ±0.10%) were placed in the pure bending zone, whereas LVDT1 and LVDT2 (range of ±25 mm and a linearity error of ±0.10%) were installed between the supports and the applied load points. The load cell (maximum measuring capacity of 200 kN and a linearity error of ±0.05%)

[i] In the present context, the percentage of chlorides was defined as the ratio mass of the added NaCl in a cubic meter of water.

was placed between the actuator and the steel device that distributed the load into two equal parts. TML BFLA-5-3 strain gauges were placed along the CFRP laminate strip and on the tensile steel reinforcement, whereas TML PFL-30-11-3L strain gauges were used to monitor strains on the concrete. SG1 and SG4 were glued on the laminate near the end anchorage (30 mm away from the plate anchor – MA; 630 mm away from the extremities of CFRP laminate – GA), SG2 was placed on the laminate at mid-span and SG3 under the applied load point. Specimens strengthened with the GA system were also monitored with two extra strain gauges at the middle of the anchorage zones (SG1' and SG4' near SG1 and SG4, respectively). The concrete strain was assessed with a strain gauge (SG5) placed at mid-span on the top surface, and the steel reinforcement strain by means of another strain gauge (SG6) fixed in the tensile rebar positioned in the middle of the cross-section, at mid-span. In addition, crack width evolution during testing was measured through a handheld USB microscope (VEHO VMS-004D).

To document the evolution of the processes that lead to the degradation of the strengthening effect provided by the CFRP laminate, the bottom surface of the specimens at which the laminates were inserted was analysed using a Digital Image Correlation procedure [19]. The lens used had an aperture of f11 and the focal length was 36 mm. Led lights were used to illuminate the surface of the specimen. The camera sensor was a full frame size, with 36 Mpix. Considering that the priority was to trace the initiation and propagation of the cracks at the tensioned face of the specimens during testing, the principal tensile strain fields were mapped using a fine facet mesh.

2.2. Material characterization

Material characterization included the evaluation of the mechanical properties of the materials involved in this experimental program, namely: concrete, steel, CFRP laminate strip and epoxy adhesive. The ready-mixed concrete (grade of C30/37) was produced based on the proportions of mixing components by weight of 1: 2.95: 2.93: 0.02: 0.56 (cement: fine aggregate: coarse aggregate: superplasticizer: water). Aggregates were composed of crushed granite with a maximum size of 12.5 mm and Portland cement type CEM II/A-L 42,5R was used. A single batch was mixed to cast all slabs and testing samples. For characterizing the mechanical properties of the concrete, six cylindrical specimens with 300 mm of height and 150 mm of diameter were used for each series. The modulus of elasticity and the compressive strength were evaluated 28 days after casting following the LNEC E397-1993:1993 [20] and NP EN 12390-3:2011 [21] recommendations, respectively. Additionally, the modulus of elasticity and the compressive strength were also characterized at the time when the static tests of the slabs up to failure occurred (see Table 2). Results show the evolution of the modulus of elasticity (E_c) and the compressive strength (f_c) for specimens in contact with water (series TW, CW and WD), which is related to the

process of hydration of the cement [22]. When comparing the specimens fully immersed in water (series TW) with the reference series (T0), an additional increase of 20% and 35% of the E_c and f_c, respectively, were observed.

Steel rebars of type A400 NR SD with a diameter of 8 mm (∅8) and 6 mm (∅6) were used as internal reinforcement. In order to determine the tensile properties of steel reinforcement, four samples of each bar type were used. Tensile tests were carried out according to NP EN ISO 6892-1:2012 [23] recommendations and the results in terms of mean values for the modulus of elasticity (E_s), as well as yield (f_y) and ultimate (f_u) tensile strengths are presented in Table 2.

The pultruded CFRP laminate strips (Type: S&P Laminates CFK) were used in the experimental work. These composite laminate strips possess a smooth external surface and consist of unidirectional carbon fibres (fibre volume content is higher than 68%) held together by an epoxy vinyl ester resin matrix [24]. Tensile properties were assessed using six samples and the experimental procedure followed was the one described by ISO 527-5:1997 [25]. A Young's modulus (E_f) of 168 GPa and an ultimate strength (f_f) of 2944 MPa were obtained (see Table 2).

The two-component epoxy adhesive (Type: S&P Resin 220) used to bond the CFRP laminate to the concrete surface is solvent free, thixotropic and grey. Previous studies have shown that, after 7 days of curing at 21 ºC, a modulus elasticity of 8.7 GPa (CoV=6.0%) and a tensile strength of 20.7 MPa (CoV=11.0%) are obtained [26].

2.3. Strengthening procedures

The experimental program included eighteen slabs strengthened with a prestressed CFRP laminate strip. Prestress was achieved through the direct prestressing method, in which the laminate strip may be jacked against an anchor system that is mounted on the slab itself. Two anchorage systems were studied in this work: (i) the mechanical anchorage (MA), which uses the metallic plates at the end of the CFRP strip; and, (ii) the gradient anchorage (GA), in which a non-metallic anchorage is created due to the adhesive's ability to cure faster at higher temperatures. Both systems are commercially available and have been applied on site to strengthen several RC structures, being available by the same manufacturer company of the CFRP reinforcement and epoxy adhesive. As shown in Fig. 2 and Fig. 3, the MA and GA methods involve the use of common components (clamp units, guides, aluminium frame, hydraulic jack and hoses, and a manual hydraulic pump) and specific components. For instance, the metallic anchor plate is a hard-aluminium rectangular plate (200 mm × 270 mm × 10 mm) with six holes of 18 mm diameter and is used only on the MA system. The heating device is an electronic equipment with several heating

elements (100 mm × 100 mm, type 'Termofoil') and is used exclusively on the GA method [27, 28]. The strengthening procedures using the MA and GA systems, share some common application steps, mainly:

(i) Preparing the surface of the concrete substrate is the first step for both methodologies. The zone where the laminate strip is applied was sand-blasted and then cleaned with a compressed air blower. The expected average roughness (R_a) of the sand-blasted surface was 0.01 mm [9] (see Fig. 2a and Fig. 3a);

(ii) Several holes were drilled to accommodate temporary and permanent bolt anchors. The average drill hole had a depth of 85 mm and was cleaned with an airbrush after drilling. GA system involves temporary bolts only, while for the case of the MA system, six M16 8.8 permanent bolt anchors (stainless steel) were used to fix each metallic anchorage plate. A chemical bond agent (HIT-HY 200-A®) was used to fix these bolts to concrete (see Fig. 2b and Fig. 3b);

(iii) Two metallic guides were placed in their predefined location to guide and fix the clamp units. Then, the clamp unit was placed in-between the guides at each extremity of the slab;

(iv) The CFRP laminate strip was cut with the precise length (2200 mm) and cleaned with a solvent. The epoxy adhesive was prepared according to the requirements included in the producer specifications. Subsequently, the adhesive was applied on the surface of the laminate and on the concrete surface region in contact with the laminate. The special gluing set used to apply the epoxy on the laminate guarantees a minimum thickness of 2 mm of such bonding agent (see Fig. 2c and Fig. 3c). Subsequently the CFRP laminate was placed in its final position and slightly pressed against the concrete substrate (see Fig. 2c and Fig. 3c);

(v) The clamping units were closed to fix the CFRP laminate strip. A torque of 170 N·m was applied to each screw using a dynamometric wrench (see Fig. 2d and Fig. 3d);

(vi) The metallic anchor plates and the heating device were placed in their predefined locations for the case of the MA (see Fig. 2e) and GA (see Fig. 3e) systems, respectively. It should be pointed out that the metallic anchor plates were always slightly grinded with sandpaper and cleaned with a solvent;

(vii) Aluminium frames were placed at their predefined positions and fixed against the concrete substrate with anchors to accommodate the hydraulic jack (see Fig. 2f and Fig. 3f);

(viii) Eventually, the hydraulic jack was installed on the aluminium frame and, using a manual hydraulic pump, the prestress was applied to the CFRP laminate strip (see Fig. 2g and Fig. 3g).

After the prestress application on the CFRP strips (see Fig. 2h and Fig. 3h), different procedures were followed for MA and GA systems. In the MA system, each bolt anchor of the metallic anchor plates was tightened with a torque of 150 N·m in order to increase the confinement provided by the metallic plates at the anchor's region and reduce the probability of the CFRP laminate to slide at the ends. Additional fixing screws were mounted between the frame and the clamp units in order to block the prestressing system and, consequently, avoid prestress losses during the curing of the adhesive. The strengthening application was concluded after approximately 24 hours. Finally, the equipment was removed (fixing screws, clamp units, guides and aluminium frames) and temporary anchors and the CFRP laminate outside of the anchor plates were cut off.

Within the scope of the present work, gradient anchorages of 600 mm in length, composed of three sectors (50 mm wide and 200 mm long each) were used. During the application of the gradient, the specimens were always monitored in terms of applied force by the hydraulic jacks and temperature at the distinct sectors composing the heating devices. The evolution of the temperature, jack force and strain over time are represented in Fig. 4: the first sector was heated to 160ºC for a period 15 minutes, followed by an exponential temperature decrease during 20 minutes (down to 120ºC), and finally by a cooling phase. In the following sectors the same heating process was carried out 10 minutes after the beginning of the cooling phase of the previous one. Approximately 15 min after the initiation of the cooling phase of each sector, 1/3 of the total applied force was released. This waiting time was chosen in order to ensure that the epoxy adhesive has cooled down to temperatures below 50ºC.

The prestress level was controlled by strain gauges previously placed at the mid-span of the CFRP laminate strip. The average prestrain imposed was approximately 0.4%. Table 1 shows the values of the registered prestrain and prestress force at the middle of the CFRP laminate for all specimens at the end of the strengthening procedure.

A schematic schedule representing the main tasks performed during this work is shown in Fig. 5. Approximately six months after the strengthening, the slabs were exposed to the different studied environmental conditions. Initially, the prototypes were placed in the empty water tanks, or inside a climatic chamber in the case of the slabs REF. In each tank, or climatic chamber, four slabs were placed: two slabs (one MA and one GA) to be subjected to the corresponding environmental condition and two others (one MA and one GA) to be subjected to the combined effect of the environmental condition and the sustained loading. Several granite blocks (weight from 0.8 kN to 4.6 kN) were used to achieve the predefined load (20 kN). While the weights were being laid, a continuous observation of the slab's bottom surface was carried out. Crack initiation was observed in all "_C" specimens for an average mid-span deformation of 1.7 mm and a load of approximately 17 kN. As shown in Fig.

5, the environmental condition were imposed approximately one month after loading and lasted for 8 months. Due to a technical problem that occurred on the air-conditioning system of the climatic chamber where the REF specimens were placed, the specimen GA_REF_C was disregarded. Finally, the specimens were removed from the exposure environments and the sustained loads were removed. One month later the slabs were tested up to failure.

3. Results and discussion

3.1 Stiffness

During the static tests the deflections along the longitudinal axis of the slabs were monitored. Fig. 6 presents the evolution of the mid-span deflection with the applied force for all tested slabs. As expected, the strengthening of the slabs with CFRP laminate significantly increased their stiffness and reduced the corresponding mid-span deflection for a specific load level. All prestressed specimens presented a delay in the crack initiation (δ_{cr}, F_{cr}) and steel yielding (δ_y, F_y) when compared to the un-prestressed specimen (see Table 3). However, no significant changes due to the use of strengthening and/or prestressing were observed regarding the stiffness of the elastic phase (K_I). This behaviour was expected considering the low amount of strengthening reinforcement used. The longitudinal steel reinforcement ratio of REF_T0 and equivalent longitudinal steel reinforcement ratio of all the strengthened slabs were equal to 0.46% and 0.53%, respectively. In average, slightly higher K_I was observed for specimens immersed in water (series TW, CW and WD) whereas the lower values were registered for the REF series. The previously mentioned results obtained for concrete's elastic modulus (see Table 2) support these observations. Results show that the uncracked concrete's contribution to the overall slabs stiffness is, by far, the largest. Also, specimens subjected to sustained loading (series "_C") appear to have a similar behaviour to the uncracked series ("_U") during the initial stages of testing: Fig. 6d and Fig. 6e show that the cracking stabilization only occurred for a load level of around 27 kN; before that, the contribution of the concrete for the initial slab's stiffness seems to be more relevant, since all environmental conditions that include water exposure (series TW, CW and WD) led to higher stiffnesses. In contrast, MA_REF_C presents the lowest initial stiffness, which can be explained by the lower stiffness and most likely the lower tensile strength of concrete that was not immersed in water.

The overall stiffness at cracked stage (K_{II}) of the strengthened slabs is substantially less influenced by the mechanical properties of the concrete. For that reason, higher K_{II} values were obtained for all strengthened slabs,

in contrast to the observed for the REF_T0 (unstrengthened slab). For the same reason values of K_{II} are relatively similar for all strengthened specimens.

In general, all prestressed slabs presented similar behaviour, which clearly means that the anchorage system type and the environmental exposure did not have a noticeable influence in the development of the deformations with the applied force. As expected, the sustained loading altered the initial deformation state of the slabs prior to static testing. As shown in Fig. 6, cracked specimens (series "_C") exhibited yielding and failure at lower deformation values, when the residual deformation obtained prior to static testing is disregarded.

3.2 Crack evolution and failure modes

As previously referred, the crack width was assessed through the use of a handheld USB microscope during the execution of the static tests. For that purpose, the first three cracks visible by naked eye located in the pure bending zone were selected based on the following criteria: one at the mid-span and other two near the load application points. The average crack width evolution was obtained from the microscope images and measured in three distinct places of each single microscope photo, as depicted in Fig. 7a. The evolution of the average crack width *versus* the applied force is plotted in Fig. 7b-f. It should be noted that in the case of series "_C", the crack width was measured since the onset of the static tests because several cracks were already visible.

Results show that the strengthening influenced the crack width increase with the applied force: for a specific load level, strengthened slabs exhibited lower crack widths when compared to the REF_T0 specimen. Prestress changed the onset of cracking by increasing the first-cracking load, at an average growth of 89% when compared with the EBR_REF_T0. Crack measurements support the previous statement. In fact, Fig. 7 shows that for the same load level, the prestressed specimens exhibit lower average crack widths. Both anchorage systems presented similar performance. The trend of crack width measurements observed for the control specimens (MA_REF_T0 and GA_REF_T0) was similar to the one observed for the uncracked specimens.

The different exposure environment conditions seemed to have no significant influence on the crack width evolution. In spite of that, specimens subjected to environments TW, CW and WD appeared to have an even lower crack width growth with the load increments. Conversely, specimens subjected to sustained loading showed a different crack width evolution: the linear regression shows a higher slope when compared to the ones relative to the remaining strengthened slabs.

A study on the crack pattern and crack spacing was carried out for all specimens. Fig. 8 illustrates the final crack pattern on the lateral surface and the average crack spacing and Fig. 9 shows the final crack pattern on

the bottom surface. The average crack spacing was measured on the bottom surface of the slabs along two lines parallel to the longitudinal axis, each of these 150 mm away from the lateral face of the slab. As expected, the results clearly showed a crack spacing reduction due to strengthening and an even greater reduction when the strengthening was prestressed. For both prestressing systems the average crack spacing decreased and, consequently, the number of cracks increased. However, the MA and GA systems produced different effects on the final crack pattern. The gradient anchorage allowed the formation of cracks along the gradient zones (occupying approximately 2/3 of these zones) and between these regions. The cracks over the gradient zone indicate that the CFRP laminate is mobilized throughout its entire length. The MA slabs presented a crack pattern that developed between the anchorage plates. The absence of cracks over the anchorage zones is related to the confinement produced in this region by the anchoring devices. As mentioned before, a torque of 150 N×m was applied in each of the six bolts that fix the CFRP laminate to the concrete with the metallic anchor plate, confining the laminate and the surrounding concrete substrate, in addition to the complementary reinforcement provided by the bolts themselves.

As previously stated, REF_T0 is an unstrengthened specimen that was tested at the onset of the environmental condition exposure. The test was stopped once the mid-span deflection reached 100 mm, the maximum deflection that can be registered by the LVDT. Concrete crushing at the top fibre would most likely be the expected failure mode (according to a section analysis, concrete crushing was expected for a load level close to 28 kN, when the strain of the steel in tension reaches 3.3%. The analysis was based on the assumption of a rectangular stress distribution in the compressed concrete region, as suggested by Fib [29]). The strengthened slabs exhibited two distinct failure modes: (i) strip debonding and (ii) CFRP tensile rupture in unidirectional tension. The MA_REF_T0 failed by CFRP rupture in unidirectional tension when the strain in the laminate strip was 1.48% (see Table 3 and Fig. 11a). As in most slabs strengthened using mechanical anchorage, failure in the MA_REF_T0 did not occur immediately after the strip debonding, since the CFRP strip was held at both ends by the mechanical anchorages. As shown in Fig. 10e, the observed debonding of the CFRP strips in MA slabs occurred in two phases: in a first stage deboning occurred near one of the two anchorages, and after a while the same happens in the anchorage placed at the opposite side of the slab. Due to this behaviour, the strains at the CFRP strip near the anchorages suddenly increased and almost reached the mid-span strain. From this point onwards the CFRP laminate strip behaved as an unbounded reinforcement, with minor strain variations along the strip length caused by the friction and interlock developed at the debonded region. Eventually, the strip was pulled out from the mechanical anchorage as shown in Fig. 11c. Digital image correlation (see

Fig. 12/Video 1) clarifies that the debonding process of the MA slabs is caused due to flexural cracks. The observed intermediate debonding was cohesive at the concrete and started with the formation of flexural cracks at mid-span of the slab that propagated towards the ends. In

Fig. 12/Video 1, it's possible to see primary flexural cracks and, when higher load levels are achieved, secondary shear cracks due to the CFRP reinforcement. All specimens with gradient anchorages exhibited a brittle failure, as in this case no mechanical end-fixing existed to provide additional anchorage. Because the strip detachment developed rapidly and very sudden, it is difficult to clearly identify the exact failure mode: although it seems that intermediate debonding caused by flexural cracks promoted the detachment of the CFRP in the GA specimens (see Fig. 13/Video 2), failure could also have started from the anchorage at the CFRP/epoxy interface and then propagate towards the middle of the concrete substrate. Fig. 9 shows flexural cracks across the gradient anchorage and they might have been the trigger that caused the failure. Nevertheless, considering the GA slabs, the strip end where the detachment started failed at the CFRP/epoxy interface, whereas cohesive failure in the concrete was observed for the remaining CFRP strip (see Fig. 9). Details regarding the influence of the anchorage systems on the structural behaviour will be discussed further in the subsequent section.

3.3 Influence of prestressing

As previously stated, literature points out several advantages deriving from the prestressing of FRP materials. In this research the average level of prestress load reached was about 40 kN, resulting in a tensile stress of about 680 MPa in the CFRP laminate strip. When prestressed slabs are compared with the un-prestressed specimen (EBR_REF_T0), a relatively small increase on the stiffness K_I and K_{II} (about 19% and 11%, respectively) is observed. Nevertheless, the first-cracking, yielding and failure loads increased substantially (approximately 90%, 30% and 31%, respectively) and, as a result, for the same load level, these specimens exhibited smaller deflections (see Table 3).

One of the main advantages of using prestressed externally bonded FRP materials for strengthening existing structures is the reduction of the existing deflections and crack widths. In the experimental programme, when the sustained loading was removed, the majority of the cracks have closed and became invisible to the naked eye. Strengthening using prestressed FRP materials may be regarded as a way to partially or totally cancel the effect of sustained loads, and consequently as a way to improve both crack width and deflection reduction.

Prestressed slabs exhibit a more efficient use of the mechanical properties of both the concrete and the CFRP: the average concrete strain in the top surface at failure of the slab was approximately 0.20%, and the CFRP

strain, ε_{fmax}, was approximately 1.18%. In contrast, immediately before failure, the concrete and CFRP strains registered in the EBR_REF_T0 specimen were 0.13% and 0.76%, respectively (see Table 3).

3.4 Mechanical *versus* gradient anchorage

The anchorage system plays an important role on the effectiveness of the prestressing technique, allowing a proper transfer of high shear stresses from the strip ends to the concrete [30]. In the case of the mechanical anchorage (MA) system, hard aluminium plates avoid the premature peeling-off of the CFRP strip by holding the laminates extremities and, in the particular case of this experimental program, by increasing the concrete's shear strength at the substrate surface due to the confinement provided by the torque applied on each anchor bolt fixing the plates. Alternatively, the gradient anchorage (GA) gradually reduces the prestressing force over several gradient segments towards the ends of the strip, eliminating the risk of premature debonding failure. However, during the monotonic tests the major difference between the behaviour of slabs with the two different anchorage systems was observed after steel yielding, when the CFRP strip debonding seems to initiate. After yielding, the steel reinforcement contribution to the increase of the slabs load carrying capacity is limited, thus making the CFRP material the greatest responsible for carrying the additional load increments. Promoted by the flexural cracks at the intermediate zone of the slab, strip debonding initiated when the load level was close to 55 kN and 56 kN for the MA and GA slabs, respectively. It should be highlighted that with the GA system the initial debonding process quickly progressed into the complete strip detachment. For the majority of the MA specimens, strip debonding produced two sudden load drops in the F-δ responses (see Fig. 6a, Fig. 6b and Fig. 6d), each drop relative to the strip detachment at each of the two extremities. Once completely detached, the CFRP strip continues to carry additional loading as an unbounded external reinforcement fixed by the metallic plates. In average the MA system allowed reaching an ultimate load of 59 kN (6.2% higher than the one observed with the GA system) and an ultimate mid-span deflection of 86 mm (GA slabs presented an average ultimate mid-span deflection of 73 mm). In essence, both anchorage systems presented similar behaviours until the yielding of the steel reinforcement. Then, for similar load/deflection levels the initiation of strip debonding led to the failure of the GA system and to the CFRP strip detachment in the MA system. Although the majority of the MA slabs presented a ductile behaviour by allowing larger deflections and greater load levels, in some cases (specimens MA_W_U, MA_CW_C and MA_WD_C) failure was observed shortly after the strip debonding initiation.

3.5 Influence of environmental condition

As referred, four environmental conditions were considered to evaluate the durability of the studied strengthening systems: (i) reference environment (REF); (ii) water immersion in tank at 20 ºC of temperature (TW); (iii) water immersion in tank with 3.5% of dissolved chlorides at 20 ºC of temperature (CW); and (iv) wet/dry cycles in a tank with water at 20 ºC (WD). As mentioned before, the concrete mechanical properties changed differently with each environmental condition. Likewise, results indicate that the properties of the epoxy adhesive might have changed thought the 8 months' exposition to these environments. In fact, a recent study [15] with the same epoxy adhesive under the same environment conditions (REF, TW and CW) has shown a decrease on the elastic modulus (about 14%, 43% and 34% for the REF, TW and CW respectively) and a decrease on the strength (about 6%, 38% and 30% for the REF, TW and CW respectively) after eight months of exposure. In contrast, Fernandes *et al.* [31] have shown that the CFRP tensile properties suffer negligible losses when subjected to full immersion in water (about 3% and 2% for the tensile strength and E-modulus, respectively) or to full immersion in water with 3.5% of chlorides (about 7% and 1% for the tensile strength and E-modulus, respectively) for a period of time that lasted up to 720 days. Because all materials properties changed differently with each environmental condition, the overall behaviour of each composite system (RC slab/epoxy adhesive/CFRP laminate strip) also changed. For all four environmental conditions a decrease on the first-cracking, yielding and ultimate loads for both MA and GA specimens was observed. When compared to the reference specimens (MA_REF_T0 and GA_REF_T0), all aged specimens presented a reduction on the ultimate parameters (in average the ultimate load, deflection and CFRP strains decreased 8.4%, 28.4% and 11.9%, respectively). In both anchorage systems the epoxy adhesive can be one of the crucial factors for its success. The deterioration of the adhesive's adherence and tensile properties seems to be the major reason for the earlier debonding initiation on the aged specimens. Regarding the GA specimens, the strip detachment always occurred at lower load levels, even in the less aggressive environmental conditions for the adhesive (CW). The lowest ultimate loads and deflections (F_u=53.52 kN and δ_u=38.21 mm) were observed for the environment REF (GA_REF_U). The MA_REF_T0 and the remaining MA slabs presented similar load levels at the onset of the strip's detachment. The MA slab subjected to the full immersion in water presented the most significant degradation. These results are in agreement with the evolution of the mechanical properties of the epoxy adhesive in time: the environmental actions TW and CW resulted in the most signifficant decrease in terms of the mechanical properties of the adhesive.

For each strengthened slab, three ductility parameters were calculated to evaluate the influence of each environmental condition on the ductility of the slab (see Table 3). In general, the increase of force (F_{max}/F_y),

deflection (δ_{max}/δ_y) and curvature (φ_{max}/φ_y) ratios between the yielding and the failure stages was higher for MA specimens. The MA_REF_T0 presented the highest ductility parameters (F_{max}/F_y =1.33, δ_{max}/δ_y=3.15 and φ_{max}/φ_y=2.13) and similar results were observed for MA slabs exposed to REF, CW and WD environments. Again, the immersion in water (series TW) resulted in the highest ductility reduction for MA specimens, being the ratio δ_{max}/δ_y of specimen MA_TW_U 49% lower than the one obtained for MA_REF_T0. This observation may be justified by the degradation experienced by the epoxy adhesive when exposed to certain environments [15]. Specimens prestressed with the GA system presented the highest ductility parameter on series TW and CW.

3.6 Influence of sustained loading

In real-life situations, a RC structure can be subjected to combined effects of physical and environmental factors, which in some cases may be synergetic. In order to evaluate their influence, as previously referred, a sustained load of 20 kN was applied simultaneously to the four studied environments. The sustained load led to the pre-cracking of all specimens allowing a greater exposure of the reinforcement and strengthening elements to the environmental conditions and, as a consequence, the greater degradation of the composite system. During the sustained loading, the maximum deformation of the slab almost reached 10 mm and cracks were visible by naked eye. When loading was removed, more than 50% of the previously reached deformation was recovered.

During the static tests, a sudden stiffness loss was observed when the applied load was close to 25 kN indicating that the cracking process was not stabilized during the application of the sustained load. Up to this point, the stiffness of the slab assumed an intermediate value between the stiffness K_I and K_{II} of the "_U" specimens. As shown in Table 3, the sustained load and consequent cracking did not have a significant influence on the ultimate behaviour. In the static tests, the failure occurred for the same load level as for the "_U" slabs but, as expected, for lower deflection values (23.6% and 6.4% lower for the MA and GA systems, respectively). For the specimens subjected to the sustained loading the separation between the debonding initiation stage and the anchorage slippage stage has decreased, reducing the ductility. Ductility parameters presented in Table 3 can quantify the reduction of the slabs ductility due to the effect of the synergies between sustained loading environmental conditions exposure. The GA specimens (GA_TW_C; GA_CW_C and GA_WD_C) presented similar ductility parameters to those obtained to the GA_REF_T0. However, all "_C" specimens strengthened with the mechanical anchorage showed significant ductility reductions. The lowest F_{max}/F_y, δ_{max}/δ_y and φ_{max}/φ_y ratios for the MA slabs were observed for series TW (F_{max}/F_y = 1.14), WD (δ_{max}/δ_y = 1.64) and TW (φ_{max}/φ_y = 1.67), respectively. In this matter, the less damaging synergy

comprehended the sustained loading and the REF environment. Yet, the MA_REF_C showed a decrease higher than 20% in each of its ductility parameters when compared to the MA_REF_T0.

In summary, the ductility of each slab was evaluated through three parameters (F_{max}/F_y, δ_{max}/δ_y and φ_{max}/φ_y) and three major factors have been observed: (i) specimens strengthened with the GA system showed minor variations in their ductility parameters after being exposed to the different environmental conditions solely (series "_U") or combined with the sustained loading (series "_C"); (ii) the ductility of MA specimens on series "_U" and "_C" was considerably lower than the ductility observed on slab MA_REF_T0; and (iii) the combined effects (sustained loading + environmental action) produced a more severe effect on the ductility reduction of MA specimens than the exposure to each environment separately.

4. Conclusions

This work presented an experimental program in which the main objective was to assess the durability of RC slabs strengthened with prestressed CFRP laminate strips using two different anchorage systems: the mechanical anchorage (MA) and gradient anchorage (GA). During eight months, sixteen slabs were subjected to the effect of four environmental conditions (reference environment - REF; immersion in tap water at 20 ºC - TW; immersion in water with 3.5% of chlorides - CW; and wet/dry cycles in tap water at 20 ºC - WD). Additionally, half of these specimens were subjected to a sustained load of 20 kN. Out of the presented results, several conclusions can be drawn:

- In general, prestress allowed higher CFRP strains at failure, thus a better use of the involved materials;
- A similar response was observed for both anchorage techniques, but the mechanical anchors of the MA system prevented a premature failure and allowed the slabs to support greater ultimate loads and deflections;
- For the GA specimens, the initial debonding process was rapidly transformed into the complete strip detachment, resulting in a brittle failure, similar to conventional externally bonded reinforcement without any end-anchorages;
- The MA_REF_T0 slab was the only that failed by CFRP rupture at its maximum tensile capacity, whereas the remaining strengthened slabs seemed to have failed by strip intermediate debonding from the concrete;

- The exposure to water (series TW, CW and WD) improved the concrete strength and the corresponding modulus of elasticity, which increased the initial slabs' stiffness and delayed the crack initiation;
- All tested environmental conditions led to a reduction of the yielding and the failure loads for both anchorage systems, but the influence of each environment was different on each anchorage system: TW and REF environment conditions seemed to have the highest degradation influence over the MA and GA slabs, respectively;
- Debonding initiation on both systems was observed at earlier test stages for specimens exposed to all environments. The main reason resides in the fact that the epoxy adhesive's properties are susceptible to degradation when exposed to humidity or water;
- The ductility of all strengthened specimens was evaluated through three ductility parameters. In general, all tested exposure environments led to a reduction of the MA slabs ductility, especially in the case of cracked specimens. The MA specimens presented the lowest ductility after the immersion in water (series TW);
- The sustained loading amplified the effect of each environmental action. This effect was more pronounced on MA specimens, which presented lower structural ductility when comparing the deflection between failure and yielding;
- The performance and ductility losses of the strengthening systems when subjected to environmental conditions and sustained loading, separately or combined, were subtle. However, considering that the tests were carried out in only 8 months, the results give clear indications towards the importance of conducting similar tests over longer periods;
- During the static tests, the control specimens (series T0) exhibit a far superior performance and ductility compared to the remaining specimens. It is clear that the study of the effects of environmental actions and sustained loading is an essential topic to truly understand the long-term properties of prestressed CFRP strengthening systems;
- Based on the obtained results it is important to, in future works, evaluate the influence of the same environmental actions for a longer period, under the influence of temperature cycles and higher concentration of salts. However, the processes used in this work has revealed great potential for the establishment of standardized procedures for durability assessment of prestressed CFRP strengthening systems.

Acknowledgements

This work was supported by the following programs: FEDER (European Funds for Regional Development) funds through the Operational Program for Competitiveness Factors – COMPETE, Operational Program for Competitiveness and Internationalization (POCI) and National Funds through FCT - Portuguese Foundation for Science and Technology under the projects FRPreDur FCOMP-01-0124-FEDER-028865 (FCT reference PTDC/ECM-EST/2424/2012), FRPLongDur POCI-01-0145-FEDER-016900 (FCT reference PTDC/ECM-EST/1282/2014) and POCI-01-0145-FEDER-007633. The authors also like to thank all the companies that have been involved supporting and contributing for the development of this study, mainly: S&P Clever Reinforcement Ibérica Lda, S&P Clever Reinforcement Company (Switzerland), Tecnipor - Gomes & Taveira Lda., Vialam – Indústrias Metalúrgicas e Metalomecânicas, Lda, Hilti Portugal-Produtos e Serviços, Lda. The first author wish also to acknowledge the grant SFRH/BD/98309/2013 provided by FCT. This paper is dedicated to Tiago Teixeira (1988–2015), former doctoral student at the ISISE R&D Research Centre at the University of Minho.

References

[1] Kim YJ, Wight RG, Green MF. Flexural Strengthening of RC Beams with Prestressed CFRP Sheets: Development of Nonmetallic Anchor Systems. Journal of Composites for Construction. 2008;12(1):35-43.

[2] Banthia N, Bisby L, Cheng R, El-Hacha R, Fallis G, Hutchinson R, et al. ISIS Educational Module 8. Durability of FRP Composites for Construction. Department of Civil Engineering, Queen's University: ISIS Canada; 2006.

[3] El-Hacha R, Wight RG, Green MF. Prestressed fibre-reinforced polymer laminates for strengthening structures. Progress in Structural Engineering and Materials. 2001;3(2):111-21.

[4] Bakis C, Bank L, Brown V, Cosenza E, Davalos J, Lesko J, et al. Fiber-Reinforced Polymer Composites for Construction—State-of-the-Art Review. Journal of Composites for Construction. 2002;6(2):73-87.

[5] Zoghi M. The International Handbook of FRP Composites in Civil Engineering: Taylor & Francis; 2013.

[6] Fib - Task Group 9.3 FRP reinforcement for concrete structures. Externally bonded FRP reinforcement for RC structures. In: (fib) fidb, editor. tecnical report. Switzerland: fédération internationale du béton (fib); 2001. p. 138.

[7] Pellegrino C, Sena-Cruz J. Design procedures for the use of composites in strengthening of reinforced concrete structures : state-of-the-art report of the RILEM Technical Committee 234-DUC. 2016.

[8] Michels J, Staśkiewicz M, Czaderski C, Kotynia R, Harmanci YE, Motavalli M. Prestressed CFRP Strips for Concrete Bridge Girder Retrofitting: Application and Static Loading Test. Journal of Bridge Engineering. 2016;21(5):04016003.

[9] Correia L, Teixeira T, Michels J, Almeida JAPP, Sena-Cruz J. Flexural behaviour of RC slabs strengthened with prestressed CFRP strips using different anchorage systems. Composites Part B: Engineering. 2015;81:158-70.

[10] You Y-C, Choi K-S, Kim J. An experimental investigation on flexural behavior of RC beams strengthened with prestressed CFRP strips using a durable anchorage system. Composites Part B: Engineering. 2012;43(8):3026-36.

[11] El-Hacha R, Aly MYE. Anchorage System to Prestress FRP Laminates for Flexural Strengthening of Steel-Concrete Composite Girders. Journal of Composites for Construction. 2013;17(3):324-35.
[12] Michels J, Sena-Cruz J, Czaderski C, Motavalli M. Structural Strengthening with Prestressed CFRP Strips with Gradient Anchorage. Journal of Composites for Construction. 2013;17(5):651-61.
[13] Aram MR, Czaderski C, Motavalli M. Effects of Gradually Anchored Prestressed CFRP Strips Bonded on Prestressed Concrete Beams. Journal of Composites for Construction. 2008;12(1):25-34.
[14] Nordin H, Täljsten B. Concrete Beams Strengthened with Prestressed Near Surface Mounted CFRP. Journal of Composites for Construction. 2006;10(1):60-8.
[15] Silva P, Fernandes P, Sena-Cruz J, Xavier J, Castro F, Soares D, et al. Effects of different environmental conditions on the mechanical characteristics of a structural epoxy. Composites Part B: Engineering. 2016;88:55-63.
[16] Karbhari VM, Ghosh K. Comparative durability evaluation of ambient temperature cured externally bonded CFRP and GFRP composite systems for repair of bridges. Composites Part A: Applied Science and Manufacturing. 2009;40(9):1353-63.
[17] Omran H, El-Hacha R. Effects of Sustained Load and Freeze-Thaw Exposure on RC Beams Strengthened with Prestressed NSM-CFRP Strips. Advances in Structural Engineering. 2014;17(12):1801-16.
[18] El-Hacha R, Green MF, Wight RG. Flexural behaviour of concrete beams strengthened with prestressed carbon fibre reinforced polymer sheets subjected to sustained loading and low temperature. Canadian Journal of Civil Engineering. 2004;31(2):239-52.
[19] Blaber J, Adair B, Antoniou A. Ncorr: Open-Source 2D Digital Image Correlation Matlab Software. Experimental Mechanics. 2015;55(6):1105-22.
[20] E397-1993 L. Concrete - Determination of the elasticity Young modulus under compression. Portuguese specification from LNEC: LNEC; 1993.
[21] 12390-3 NE. Testing hardened concrete. Part 3: Compressive strength of test specimens. Caparica: IPQ - Instituto Português da Qualidade; 2011.
[22] Termkhajornkit P, Nawa T, Kurumisawa K. Effect of water curing conditions on the hydration degree and compressive strengths of fly ash–cement paste. Cement and Concrete Composites. 2006;28(9):781-9.
[23] 6892-1 NEI. Metallic Materials. Tensile Testing. Part 1: Method of test at room temperature. Caparica: IPQ - Instituto Português da Qualidade; 2012.
[24] S&P. CFRP Laminates, Technical datasheet. Seewen, Switzerland2014. p. 6.
[25] 527-5 I. Plastics — Determination of tensile properties — Part 5: Test conditions for unidirectional fibre-reinforced plastic composites. Genève: ISO - International Organization for Standardization; 1997. p. 11.
[26] Michels J, Sena Cruz J, Christen R, Czaderski C, Motavalli M. Mechanical performance of cold-curing epoxy adhesives after different mixing and curing procedures. Composites Part B: Engineering. 2016;98:434-43.
[27] Michels J, Zile E, Czaderski C, Motavalli M. Debonding failure mechanisms in prestressed CFRP/epoxy/concrete connections. Engineering Fracture Mechanics. 2014;132:16-37.
[28] S&P. Pre-stressed S&P Laminates CFK. Manual for applicators. 2010. p. 20.
[29] FIB. The fib Model Code for Concrete Structures. Model Code 2010. Lausane, Switzerland: The nternation federation for strucural concrete (FIB); 2010. p. 653.
[30] Kotynia R, Walendziak R, Stoecklin I, Meier U. RC Slabs Strengthened with Prestressed and Gradually Anchored CFRP Strips under Monotonic and Cyclic Loading. Journal of Composites for Construction. 2011;15(2):168-80.
[31] Fernandes PMG, Silva PM, Correia LLG, Sena-Cruz J. Durability of an epoxy adhesive and a CFRP laminate under different exposure conditions. In: Proceedings of SMAR2015 – Third Conference on Smart Monitoring, Assessment and Rehabilitation of Civil Structures. Antalya, Turkey, Conference 07 - 09 Sept. 2015, Conference 2015. p. 8.

Nomenclature

E_a	Average tensile modulus of epoxy adhesive
E_c	Average modulus of elasticity of concrete at slab testing day
E_f	Average elastic modulus of CFRP laminate
E_s	Average Modulus of Elasticity of steel bars
f_c	Average compressive strength on cylinder 150mm/300mm of concrete at slab testing day
F_{cr}	Force at crack initiation
f_a	Average tensile strength of epoxy adhesive
f_f	Average tensile strength of CFRP laminate
F_{max}	Maximum force
f_t	Average ultimate strength of steel bars
f_y	Average yield strength of steel bars
F_y	Force at yielding initiation
K_I	Stiffness of the slab at uncracked state
K_{II}	Stiffness of the slab at fully cracked state
δ_{cr}	Mid-span displacement at cracking load F_{cr}
δ_{max}	Mid-span displacement at ultimate load F_{max}
δ_y	Mid-span displacement at yielding load F_y
ε_{fmax}	CFRP strain at F_{max}
ε_{fp}	CFRP initial strain
φ_y	Mid-span curvature at yielding load Fy
φ_{max}	Mid-span curvature at ultimate load F_{max}

Correia, L.; Sena-Cruz, J.; Michels, J.; França, P.; Pereira, E.; Escusa, G. (2017) "Durability of RC slabs strengthened with prestressed CFRP laminate strips under different environmental and loading conditions." Composites Part B, 125: 71–88. DOI: 10.1016/j.compositesb.2017.05.047

1 **List of Tables**

5

Table 1: Experimental program

Series	**Specimen**	**Environmental condition/Observations**	**Anchorage system**	**Initial strain, ε_{fp}** [%]	**Prestress force** [kN]	**Sustained load**
T0	REF_T0	Specimens tested at the beginning of the experimental program	-	-	-	-
	EBR_REF_T0		-	0.00	0.00	-
	MA_REF_T0		MA	0.42	41.6	-
	GA_REF_T0		GA	0.40	39.6	-
REF	MA_REF_U	Specimens subjected to laboratory premises: 20 ºC and 55% of RH	MA	0.41	40.6	No
	GA_REF_U		GA	0.41	40.6	No
	MA_REF_C		MA	0.37	36.6	Yes
	GA_REF_C		GA	0.41	40.6	Yes
TW	MA_TW_U	Specimens immersed in tap water at 20 ºC	MA	0.40	39.6	No
	GA_TW_U		GA	0.41	40.6	No
	MA_TW_C		MA	0.41	40.6	Yes
	GA_TW_C		GA	0.41	40.6	Yes
CW	MA_CW_U	Specimens immersed in tap water at 20 ºC with 3.5% of chlorides	MA	0.40	39.6	No
	GA_CW_U		GA	0.41	40.6	No
	MA_CW_C		MA	0.41	40.6	Yes
	GA_CW_C		GA	0.40	39.6	Yes
WD	MA_WD_U	Specimens subjected to wet/dry cycles in tap water at 20 ºC	MA	0.40	39.6	No
	GA_WD_U		GA	0.40	39.6	No
	MA_WD_C		MA	0.42	41.6	Yes
	GA_WD_C		GA	0.42	41.6	Yes

Table 2: Materials characterization (average values)

Concrete

Series		E_c [GPa]	ΔE_c [%]	f_c [MPa]	Δf_c [%]
T0	(28 days)[(a)]	27.78 (2.9%)	-	37.32 (1.9%)	-
	(209 days)[(b)]	30.03 (-)	8.09	40.24 (0.7%)	7.82
REF	(570 days) [(b)]	26.98 (2.4%)	-2.88	39.49 (5.3%)	5.81
TW	(570 days) [(b)]	33.44 (1.3%)	20.37	50.22 (1.3%)	34.57
CW	(570 days) [(b)]	33.87 (1.1%)	21.92	45.85 (8.0%)	22.86
WD	(570 days) [(b)]	32.20 (5.1%)	15.91	48.58 (2.1%)	30.17

Steel

Bar Type	E_s [GPa]	f_y [MPa]	f_u [MPa]
Ø6	206.9 (0.4%)	519.4 (6.1%)	670.2 (5.1%)
Ø8	235.1 (4.6%)	595.9 (4.1%)	699.0 (2.1%)

CFRP

Geometry [mm^2]	E_f [GPa]	f_f [MPa]
50×1.2	167.7 (2.9%)	2943.5 (1.6%)

Notes: [(a)] Tests at 28 days; [(b)] Tests at the age of the monotonic tests of the slabs; The values between parentheses are the corresponding coefficients of variation (CoV).

Table 3: Main results

Specimen	Stiffness		Crack initiation		Yielding			Ultimate				Efficiency and ductility parameters			FM
	K_I	K_{II}	δ_{cr}	F_{cr}	δ_y	F_y	φ_y	δ_{max}	F_{max}	φ_{max}	ε_{fmax}[(c)]				
	[kN/mm]	[kN/mm]	[mm]	[kN]	[mm]	[kN]	[10^{-3} m^{-1}]	[mm]	[kN]	[10^{-3} m^{-1}]	[%]	F_{max}/F_y	δ_{max}/δ_y	φ_{max}/φ_y	
REF_T0	8.8	0.9	0.71	7.9	18.90	24.5	-	100.00[(a)]	28.1[(b)]	-	-	-	-	-	-
EBR_REF_T0	8.1	1.2	0.68	8.5	25.87	37.1	49.24	40.69	44.0	72.04	0.76	1.2	1.57	1.46	D
MA_REF_T0	10.2	1.3	1.82	17.9	26.88	50.6	48.21	84.78	67.5	102.67	1.48	1.3	3.15	2.13	F
GA_REF_T0	9.7	1.2	1.55	16.2	29.04	50.2	52.65	43.31	57.4	76.49	1.16	1.1	1.49	1.45	D
MA_REF_U	8.3	1.3	2.04	16.1	26.26	46.1	50.36	67.34	59.9	97.87	1.40	1.3	2.56	1.94	D
GA_REF_U	8.0	1.2	1.85	15.9	28.45	48.6	51.14	38.21	53.5	68.33	1.10	1.1	1.34	1.34	D
MA_REF_C	--	1.3	--	--	26.22	48.1	71.75	65.85	61.6	108.63	1.26	1.3	2.51	1.51	D
MA_TW_U	8.6	1.3	1.68	15.6	24.54	47.1	46.06	39.56	54.4	68.17	1.13	1.2	1.61	1.48	D
GA_TW_U	10.9	1.3	1.05	12.8	25.60	47.1	47.98	41.65	55.8	78.32	1.19	1.2	1.63	1.63	D
MA_TW_C	--	1.5	--	--	22.02	50.5	55.74	41.33	57.7	83.76	1.15	1.1	1.88	1.50	D
GA_TW_C	--	1.2	--	--	23.58	49.30	42.2	37.05	56.2	63.23	1.06	1.1	1.57	1.50	D
MA_CW_U	11.5	1.3	1.92	18.5	24.57	47.35	43.7	65.45	60.9	81.68	1.23	1.3	2.66	1.87	D
GA_CW_U	8.4	1.3	2.11	17.0	24.71	46.94	45.8	41.70	56.4	77.44	1.19	1.2	1.69	1.69	D
MA_CW_C	--	1.4	--	--	19.65	47.42	47.0	38.38	58.7	79.43	1.12	1.2	1.95	1.69	D
GA_CW_C	--	1.3	--	--	21.92	47.04	49.4	39.01	57.0	80.83	1.05	1.2	1.78	1.64	D
MA_WD_U	10.7	1.3	1.30	14.2	25.53	47.64	46.3	61.33	58.8	86.20	1.27	1.2	2.40	1.86	D
GA_WD_U	10.3	1.2	1.49	16.5	26.98	48.62	47.7	40.21	55.3	69.09	1.08	1.1	1.49	1.45	D
MA_WD_C	--	1.3	--	--	20.10	48.61	38.0	32.89	55.6	63.57	1.04	1.1	1.64	1.67	D
GA_WD_C	--	1.2	--	--	23.67	49.15	49.0	37.55	56.3	73.24	1.17	1.2	1.59	1.50	D

Notes: [(a)] These slabs reached the maximum pre-defined deflection without failing; [(b)] Values for the mid-span deflection of 100 mm; [(c)] The maximum CFRP strain did not necessarily occur at the mid-span; Failure modes: D = Debonding (cohesive failure at the concrete); F = CFRP tensile failure.

List of Figures

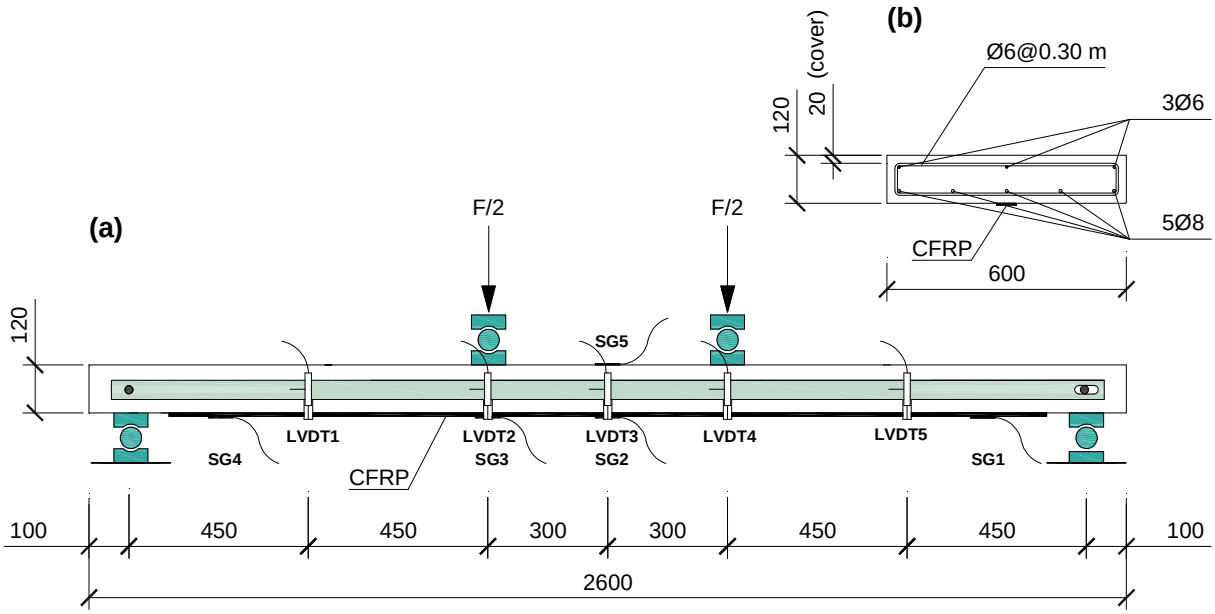

Fig. 1: Specimen's geometry and test setup. Note: all units are in millimetres.

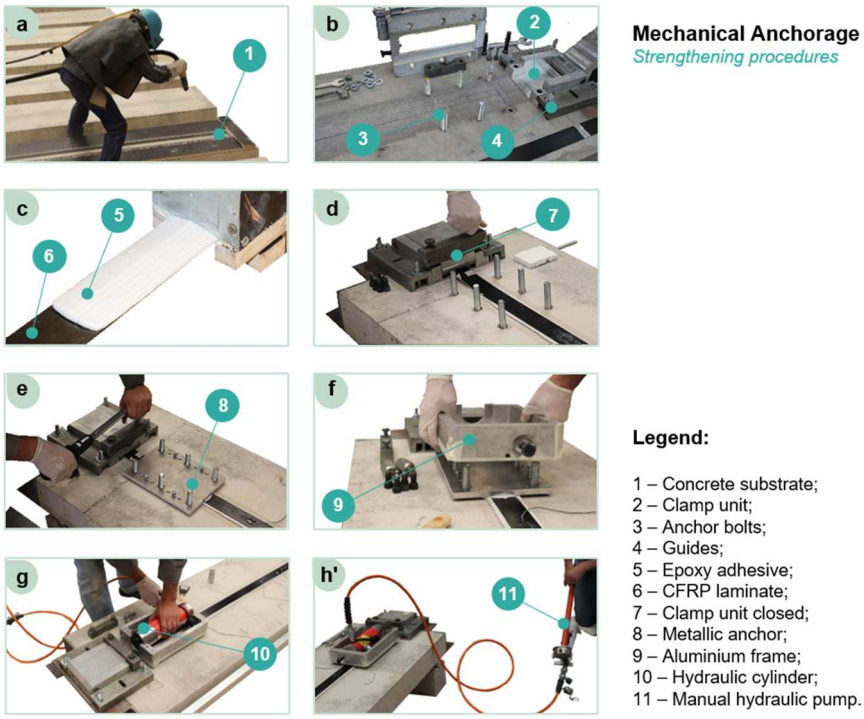

Fig. 2: Strengthening procedures for the mechanical anchorage (MA) system.

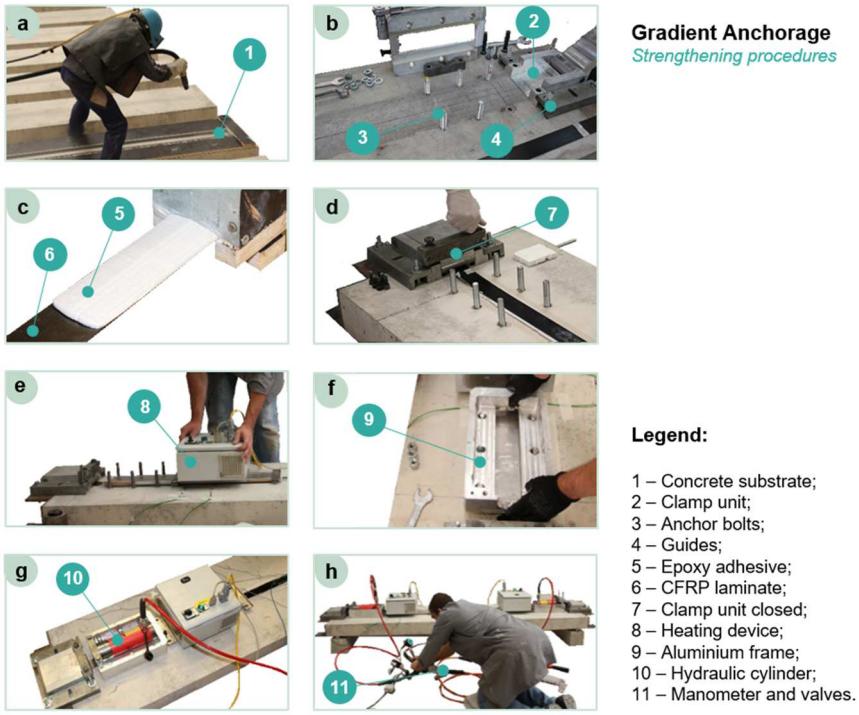

Fig. 3: Strengthening procedures for the gradient anchorage (GA) system.

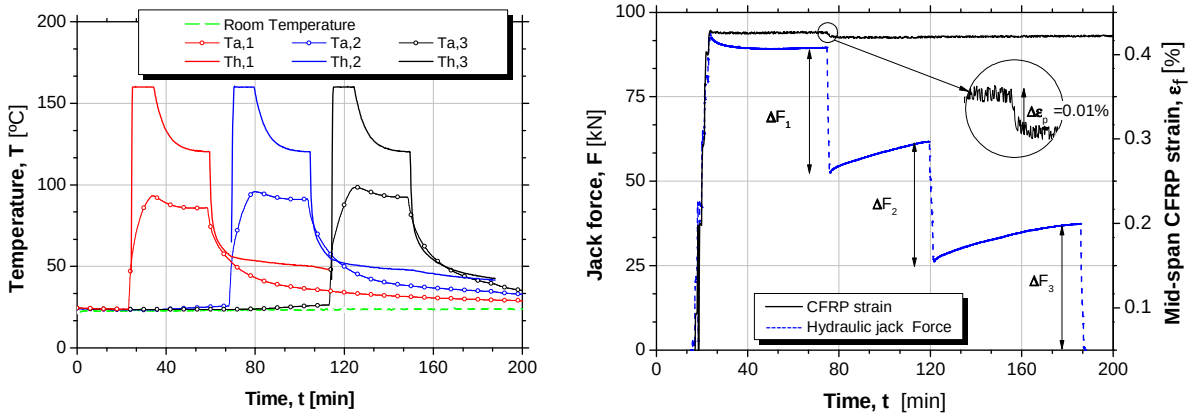

(a) **(b)**

Fig. 4: Evolution of the temperature, jack force and CFRP strain on GA_REF_T0 over time: (a) temperature in the heating elements $T_{h,i}$ and in the epoxy adhesive $T_{a,j}$; (b) hydraulic jack force F and mid-span CFRP strain ε_f.

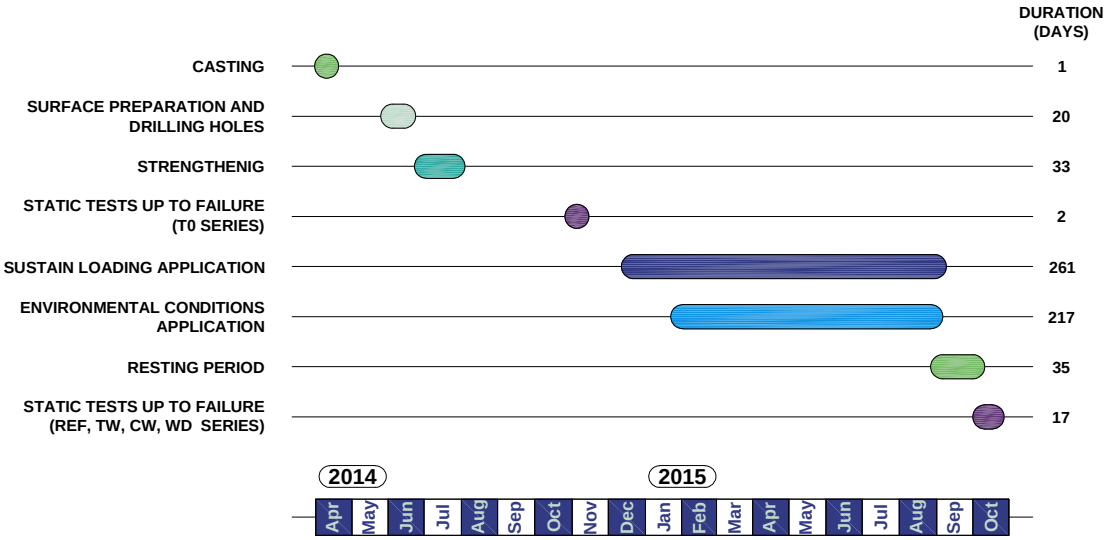

Fig. 5: Timeframe of developed work

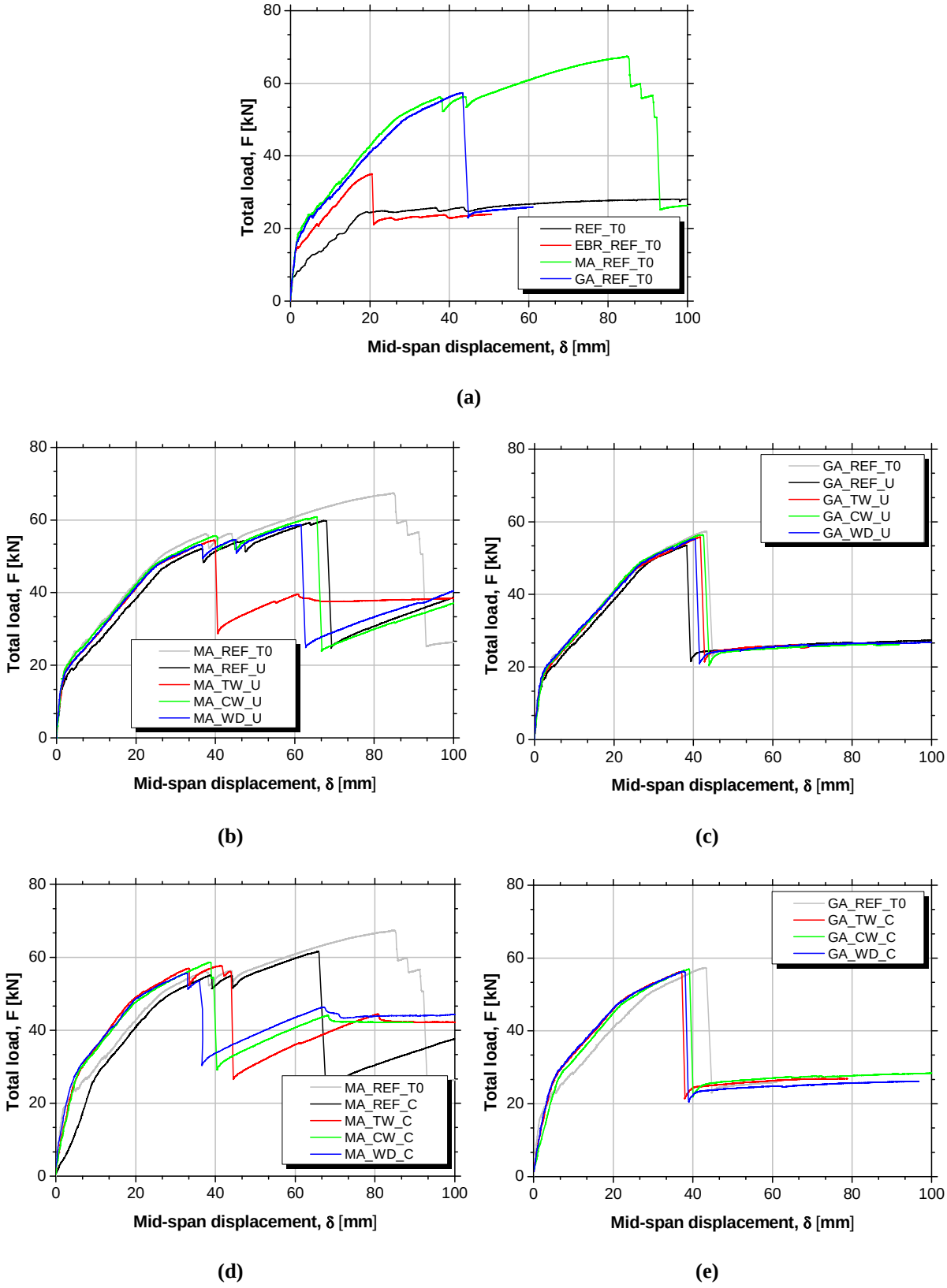

Fig. 6: Total force *versus* mid-span deflection: (a) Control specimens; (b) uncracked MA specimens; (c) uncracked GA specimens; (d) cracked MA specimens; and (e) cracked GA specimens.

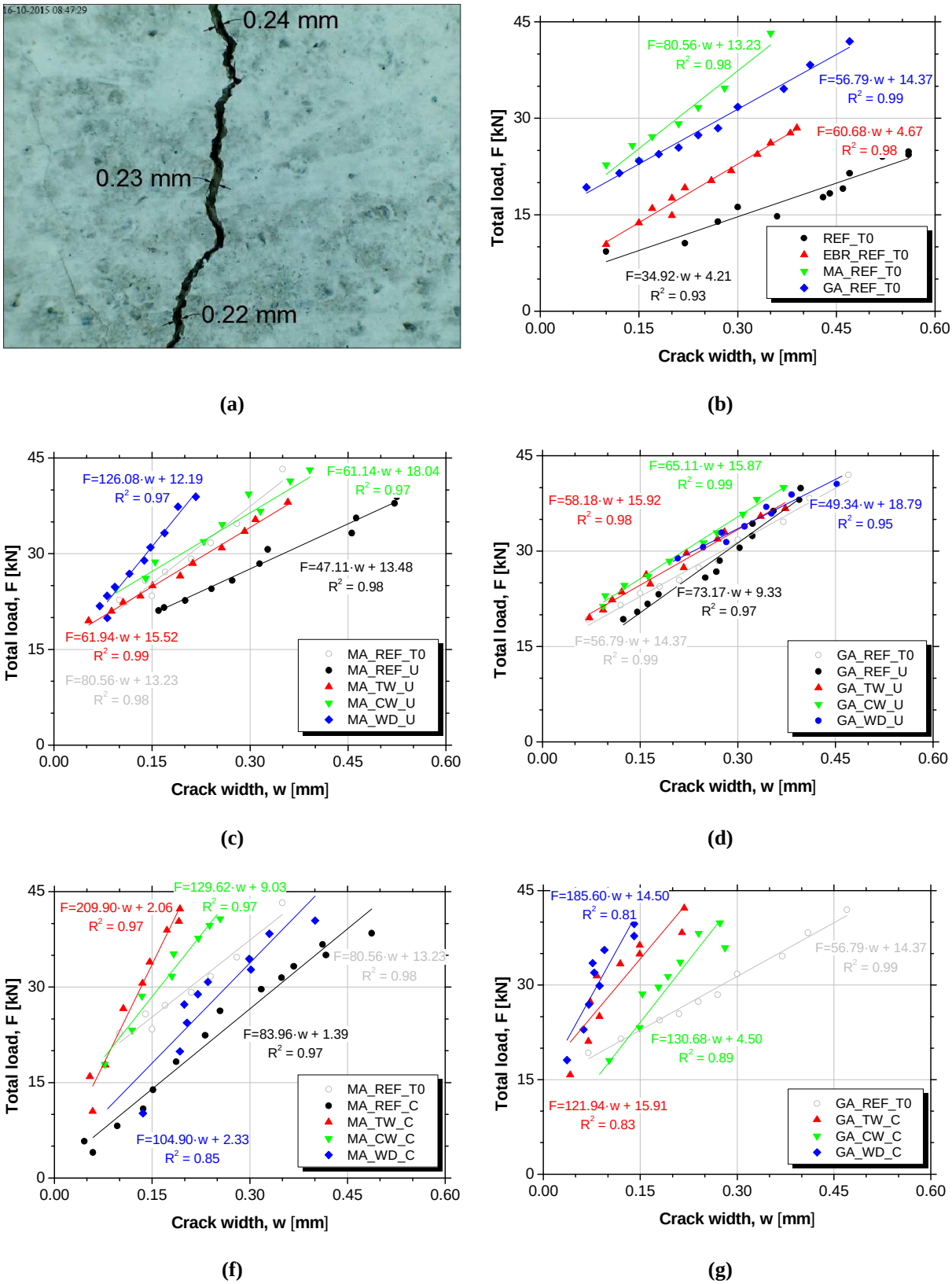

Fig. 7: Crack width evolution of: (a) Typical photo of a crack (MA_REF_U); (b) Control specimens; (c) uncracked MA specimens; (d) uncracked GA specimens; (e) cracked MA specimens; and (f) cracked GA specimens.

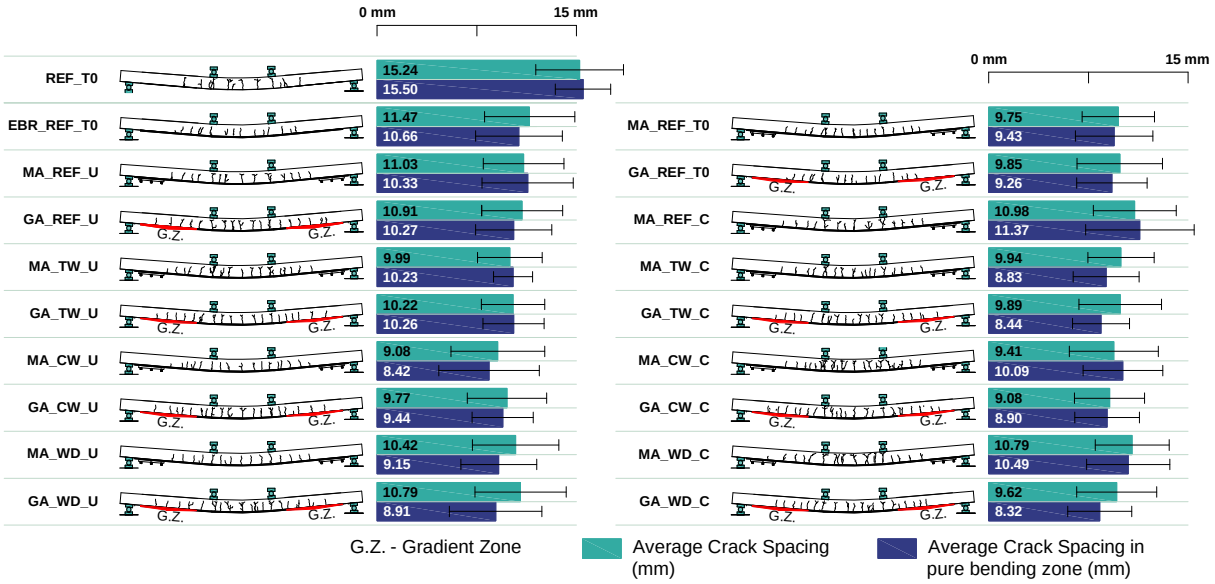

Fig. 8: Crack pattern at the end of the test of each slab and average crack spacing.

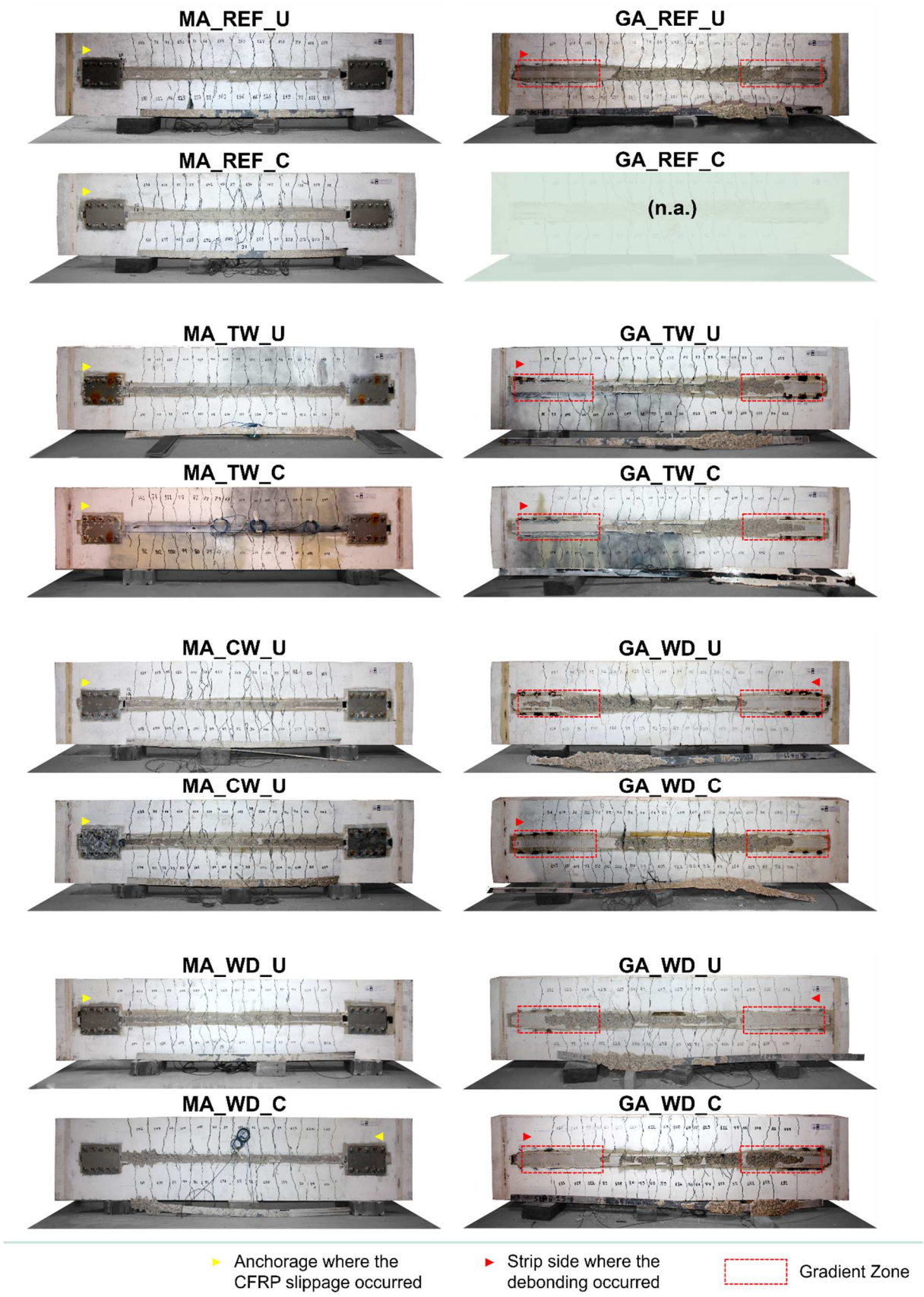

Fig. 9: Crack pattern observed on the bottom surface and failure modes.

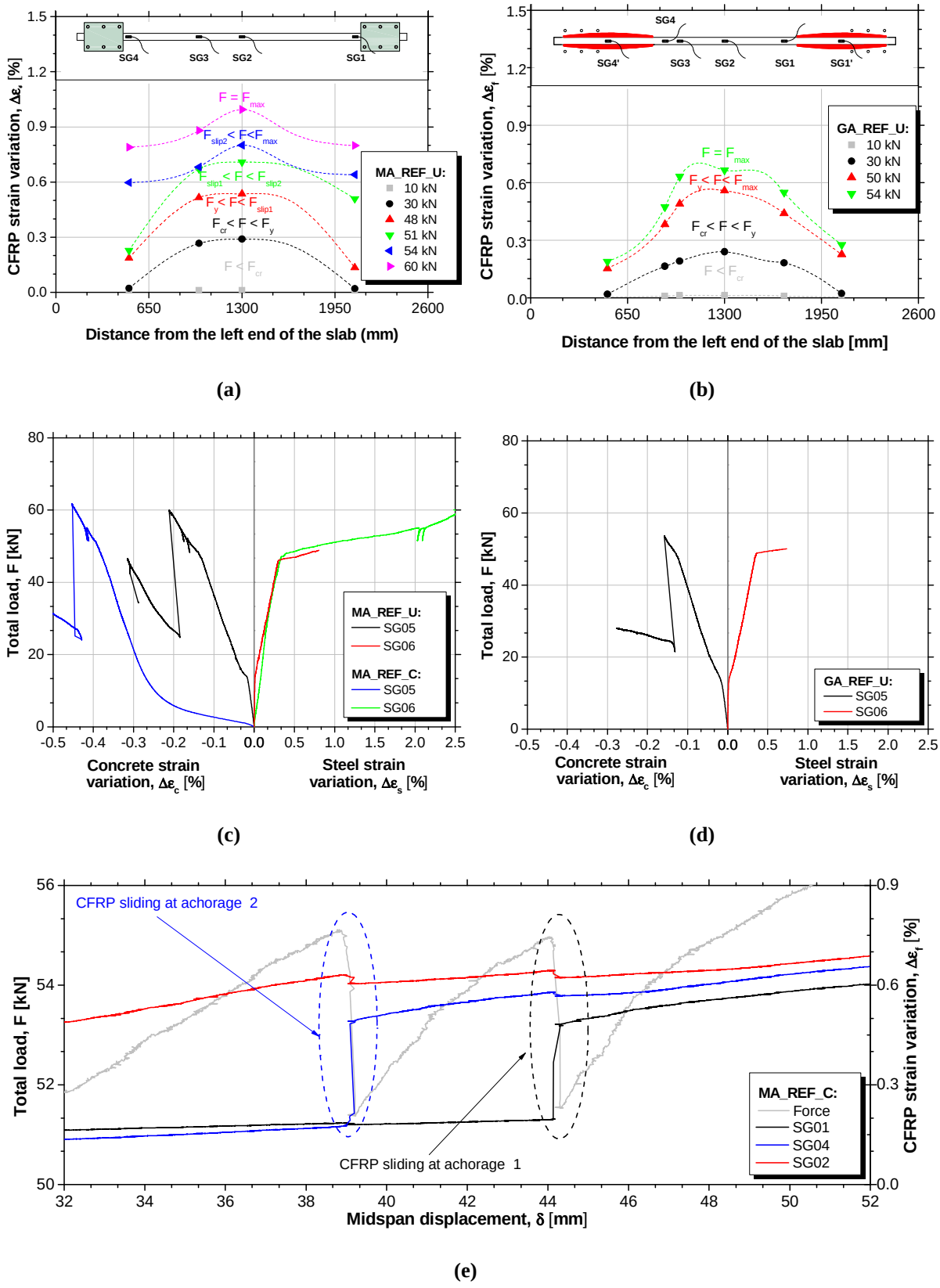

Fig. 10: Materials strain variation: (a) CFRP strain variation in MA_REF_U; (b) CFRP strain variation in GA_REF_U; (c) concrete and steel strain variation in MA_REF_U and MA_REF_C; (d) concrete and steel strain variation in GA_REF_U; and (e) CFRP sliding at anchorages for MA_REF_C.

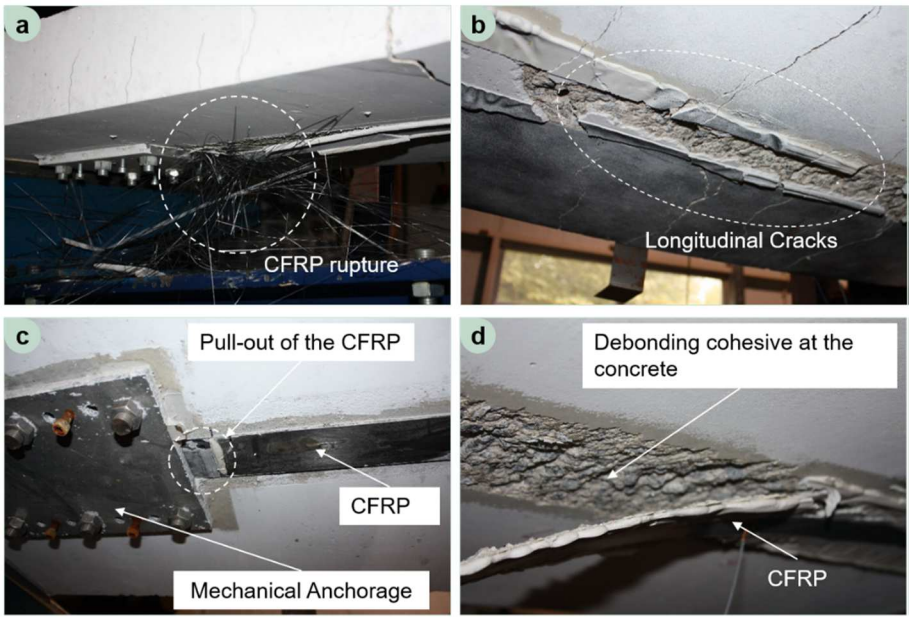

Fig. 11: Failure modes: (a) CFRP rupture in unidirectional tension (MA_REF_T0); (b) observed longitudinal cracks at the epoxy region (GA_TW_C); (c) CFRP strip pull-out from the mechanical end/anchorage (MA_WD_C); and (d) detail of a cohesive at the concrete debonding (GA_WD_U).

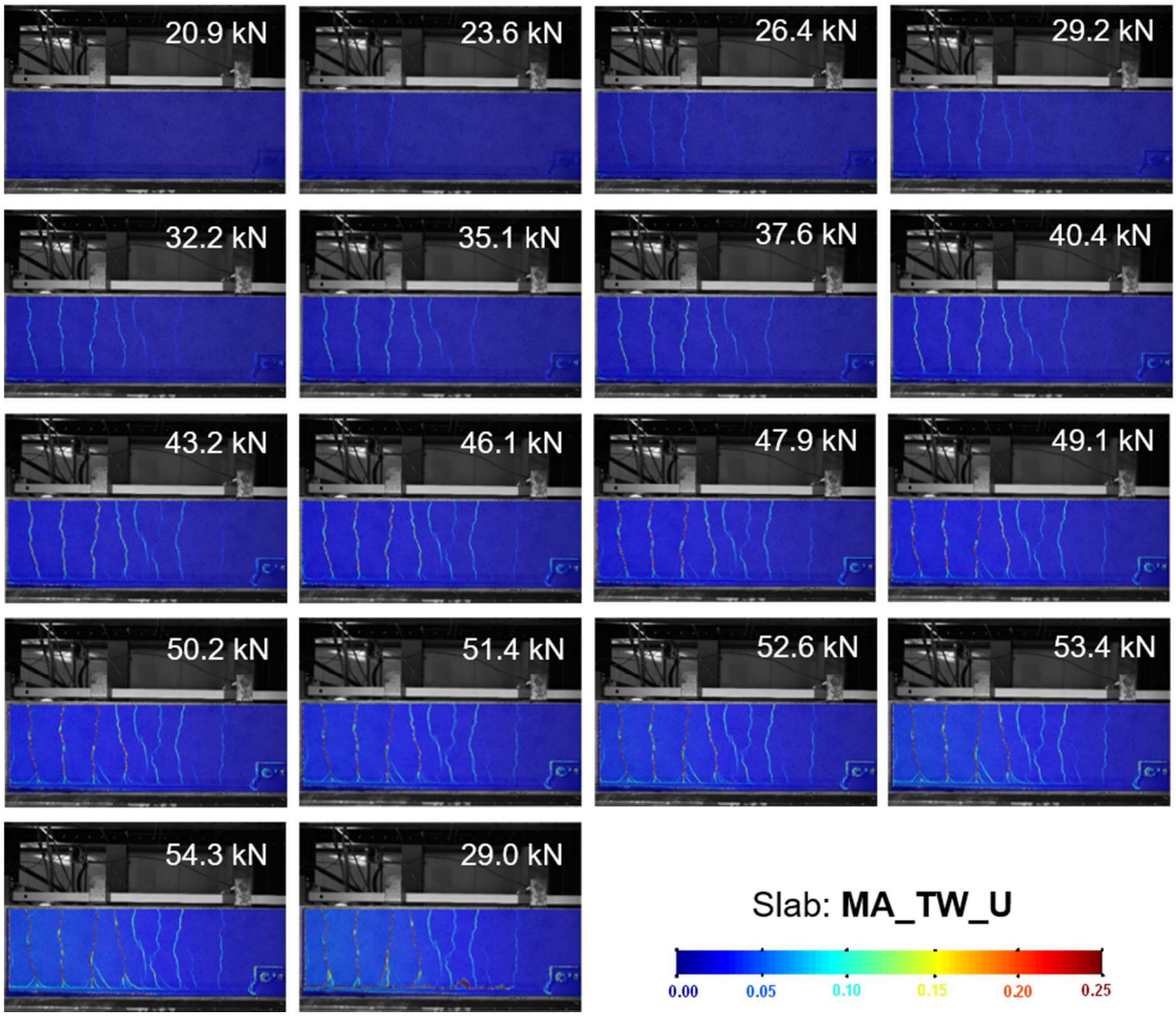

Fig. 12: Digital image correlation on MA_W_C slab (maximum principal strain field).

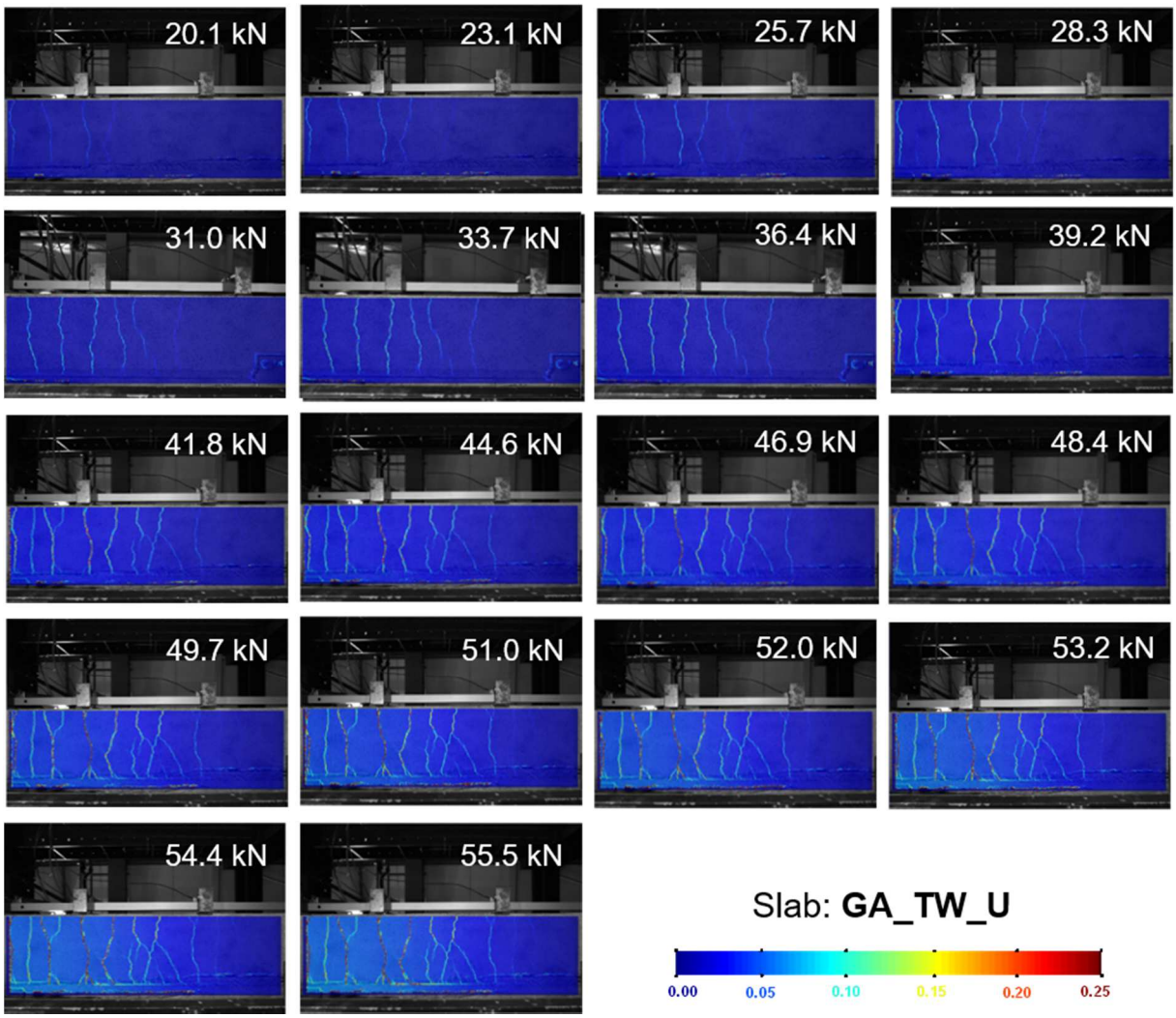

Fig. 13: Digital image correlation on GA_W_C slab (maximum principal strains).